

## RESEARCH ARTICLE

# Accumulative Imaging Method of Grounding Grid Topological Features Based on Combined Sources

XIZHE ZHANG<sup>1</sup>, BEN YU<sup>2</sup>, LONGHUAN LIU<sup>1,3</sup>, ZHIHONG FU<sup>1,3</sup>,  
JINSHAN YU<sup>2</sup>, AND XIN CHENG<sup>3</sup>

<sup>1</sup>State Grid Tianjin Electric Power Company, Tianjin 300090, China

<sup>2</sup>Electric Power Research Institute, State Grid Tianjin Electric Power Company, Tianjin 300384, China

<sup>3</sup>College of Electrical Engineering, Chongqing University, Chongqing 400044, China

Corresponding author: Longhuan Liu (20133954@cqu.edu.cn)

This work was supported in part by the Technology Projects of State Grid Tianjin Electric Power Company under Grant KJ22129, and in part by the Science and Technology on Near-Surface Detection Laboratory under Grant 6142414211607.

**ABSTRACT** One essential requirement for grounding grid state detection is quick and accurate localization of the topology. The combined source detection approach works well for increasing the signal amplitude and detection efficiency inside large grounding grids. However, the presence of bypass branch currents and grounding grid breakpoints causes variations in the location calculated by the peak approach during tiny grounding grid topology detection. The magnetic field superposition method under the excitation mode of multiple sources exacerbates this positioning error. This paper presents a topological feature accumulation imaging method designed for combined sources to address this problem. The proposed approach examines the effect of the bias in the surrounding branch current amplitudes on topological localization by utilizing the concepts of electromagnetic induction. The factors contributing to increased topological localization errors were examined by investigating the relationship between the superposition effect of the surface magnetic induction strength and localization error under different combined excitations, particularly in the context of breakpoints in the grounding grid topology. The proposed method uses the top-hat algorithm to extract top-hat features of the amplitude of the surface magnetic induction intensity under every type of excitation. Top-hat eigenvalue accumulation was used to reduce topological localization offsets by mitigating superfluous signals. The advantage of this method over conventional processing approaches is demonstrated by simulations and test field experiments, which show enhanced accuracy in combined source topological localization for small grounding grids.


**INDEX TERMS** Grounding grid, positioning biases, combined sources, top hat algorithm.

## I. INTRODUCTION

Maintaining the regular operation of electricity systems requires routine inspections of the grounding grid conditions [1], [2], [3]. However, the grounding grid topology is the primary basis for conventional techniques for grounding grid condition examination, such as the electrical network approach [4], [5] and the electrical impedance method [6], [7]. Additionally, it is important to localize faults in the

grounding grid [8], [9]. However, if there is no advance knowledge of the actual topological location of the grounding grid or to check whether the status of the grounding grid has changed, it may affect the normal operation of surface power equipment and the safety of the staff [10], [11]. Therefore, it is necessary to accurately localize the grounding grid topology at the actual substation.

The surface magnetic field method is an effective and commonly employed technique for localizing the topology of a grounding grid [12], [13]. In this method, current is injected into the horizontal grounding grid through a lead wire, and the

The associate editor coordinating the review of this manuscript and approving it for publication was Yi Ren .

surface magnetic induction strength is analyzed to localize the grounding grid topology and diagnose the breakpoints. Based on the principle of electromagnetic induction, the gradient of the horizontal and vertical components of the magnetic induction strength directly above the energized conductor reaches its maximum value. The grounding grid topology may be accurately localized by determining the location of the dummy point for the vertical component of the magnetic induction strength or the peak value of the horizontal component of the magnetic induction strength at the ground surface. Techniques such as the watershed algorithm [14], differential method [15], and wavelet analysis method [16] can be used to achieve this goal. A combined source excitation method has been suggested in the literature [17] to improve the construction efficiency. By rotating the excitation connections sequentially, this technique increases the magnetic induction intensity in a weak magnetic field area. Additionally, under combined source excitation, the superimposed magnetic field approach has been successfully used in the literature [18] to extract topological information about the grounding grid. The efficiency and precision of grounding grid maintenance operations can be increased significantly by implementing these techniques.

The grounding grid topology localization methods in the above references actually utilize various algorithms to determine the peak value of the data, but the location of the peak value of the grounding grid topology does not always represent the exact location of its topology in some typical topology arithmetic examples, which will be explained in detail in the second section of the paper. On the basis of combined source composite excitation, the method proposed in the literature directly superimposes the surface magnetic field for topology extraction [14], [15], [16], without considering the effect of superimposed magnetic field on topology offset, which affects the accuracy of topology localization of the grounded grid.

In this paper, the reasons for the topological offset are analyzed and the literature processing methods that increase the topological identification offset error are described. Then, the surface magnetic field signal characteristics of grounded grids with the presence of breakpoints are analyzed, and a method of accumulating topological features is proposed to solve the problem of the topological localization offset of the grounding grids under the excitation of the combined sources. Different from superimposing the magnetic fields under all excitations, the method improves the accuracy of topological localization of grounding grids under combined source excitations by selecting the magnetic field data with topological features among them to be superimposed, which improves the signal recognition and reduces the topological offset at the same time. Finally, the effectiveness of the algorithm is demonstrated by simulation examples and field tests. The method can improve the topological localization accuracy on top of the use of combined source equipment.

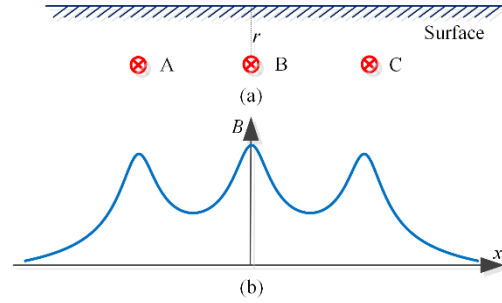


FIGURE 1. Modeling of buried parallel conductors and surface magnetic induction magnitude.

## II. EXAMINATION OF TOPOLOGICAL OFFSETS' CAUSES IN COMBINATORIAL SOURCES

Assuming a current magnitude of  $I$  flowing through a section of a branched flat steel conductor, the magnetic induction generated at any point  $P$  in space can be computed using (1), where  $\theta_1$  and  $\theta_2$  denote the angles between the line connecting the two end points of the straight wire and the spatial point  $P$  and the direction of the current  $I$ , respectively. The magnetic induction induced at a spatial point is the vector accumulation of the branch currents.

$$\begin{aligned}\vec{B}_k &= \int d\vec{B} = \int_{\theta_1}^{\theta_2} \frac{\mu_0 I \sin(\theta)}{4\pi a} d\theta \vec{e}_\phi \\ &= \frac{\mu_0 I}{4\pi a} (\cos(\theta_1) - \cos(\theta_2)) \vec{e}_\phi\end{aligned}\quad (1)$$

$$\vec{B} = \sum_{k=1}^n \vec{B}_k \quad (2)$$

where  $\mu_0$  is the magnetic permeability.  $a$  is the vertical distance from  $P$  to the conductor.  $\vec{e}_\phi$  is the unit direction vector of the magnetic field.

When employing a composite source grounding grid detection system to identify a compact grounding grid topology, the amplitude of the magnetic induction strength directly over the small grounding grid is influenced by two primary factors: the current flowing through the nearby branch and the superposition of magnetic fields resulting from various excitation combinations.

### A. EFFECT OF BYPASS CURRENTS ON TOPOLOGY OFFSETS

In Fig. 1(a), the model features parallel energized conductors denoted as A, B, and C, all of which are underground infinite-length energized conductors. When equal-magnitude currents flow through A, B, and C in the same direction, the resulting horizontal magnetic induction  $B_x$  at the ground surface is as depicted in Fig. 1(b). Every energized conductor produces a point of great magnitude near the surface directly above it, and due to the symmetry of the location and the energizing current, the magnetic induction is greatest directly above conductor B.

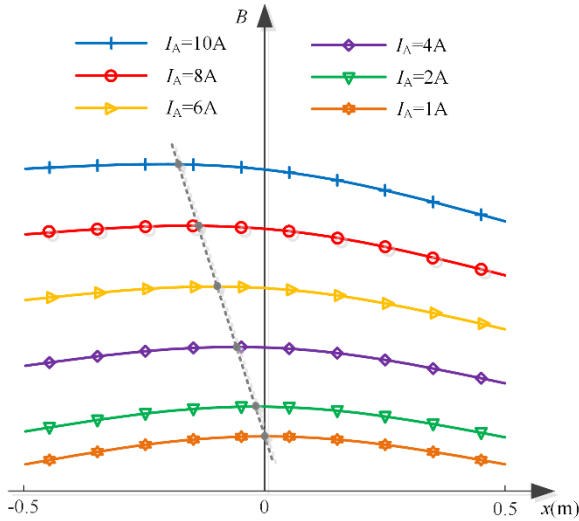


**FIGURE 2.** Magnitude of surface magnetic induction at different magnitudes of bypass branch currents.

When current is introduced into the grounding grid, variations in the circulating current among adjacent grounding grid elements often occur because of the shunt effect within the grounding grid. This phenomenon is particularly pronounced when dealing with small-mesh grounding grids. The magnetic induction strength generated by the neighboring branches influences the position of the maximum magnetic induction strength at the ground surface, resulting in topological shifts. As shown in Fig. 2, changing the current amplitude at point A in Fig. 1 changes the magnetic induction intensity in the localized region of the surface at point B, thereby affecting the position of the maximum magnitude.

As shown in Fig. 2, within a symmetrically structured parallel wire configuration, an increase in the amplitude of the energizing current on one side results in a shift in the horizontal position corresponding to the peak of the magnetic induction intensity. This shift occurred toward the side where the current amplitude was larger. Moreover, the magnitude of the position shift was directly proportional to the amplitude of the current, with larger current amplitudes causing more significant position shifts.

**B. IMPACT OF SUPERIMPOSED MAGNETIC FIELDS ON TOPOLOGICAL OFFSETS**

The operational principle of the combined source involves simultaneous connection of multiple lead wires. A predetermined order was established to select two lead wires for current injection and withdrawal, enabling comprehensive coverage of the grounding grid measurement area. In Fig. 3, breakpoints in the grounding grid model detection are evident with a grid side length of 3m and a buried depth of 0.8m. Breakpoints exist within the range ( $x = 3-6m, y = 6m$ ). Excitations AB, AC, and AD were selected to compute the magnetic induction along the horizontal measuring line ( $x =$

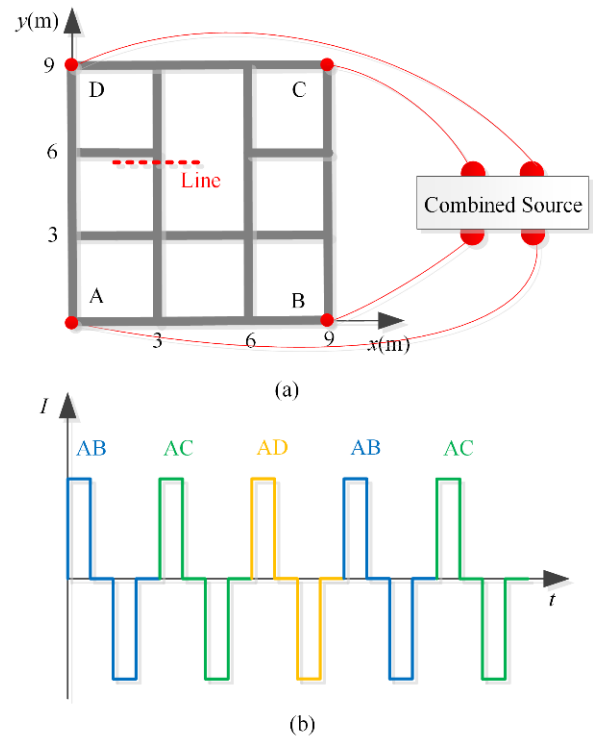


**FIGURE 3.** Combined source connection schematic and current waveform.

$2-4m, y = 5.9m$ ), as illustrated in Fig. 4(a). Under AC and AD excitations, the magnetic induction intensity attained significant values near or directly above the flat steel. However, when AB excitation was applied, the presence of a breakpoint resulted in a notable difference in the current circulation between the left and right sides of the measurement line, leading to the absence of peak characteristics near the flat steel directly above. Further, an AB excitation produces a smaller peak than AC and AD because the presence of topological breakpoints affects the branch current distribution, and there is less current circulating in the branch flat steel in the vicinity of the measurement line when the AB excitation is injected.

Given the absence of a peak feature in the magnetic induction intensity under AB excitation, the magnetic induction intensities under all excitations, as well as AC and AD excitations, were separately superimposed. The results are shown in Fig. 4(b). It is evident that superimposing the magnetic induction intensities for all the excitation combinations leads to a more significant topological offset. Notably, when only the magnetic induction intensities generated by AC excitation and AD excitation are superimposed, the result aligns more closely with the actual topology position compared with the outcome under complete superimposition. The above optimization is essentially a selection of the data containing the topological features, and the reduction of the topological offset can be achieved by this method of processing.

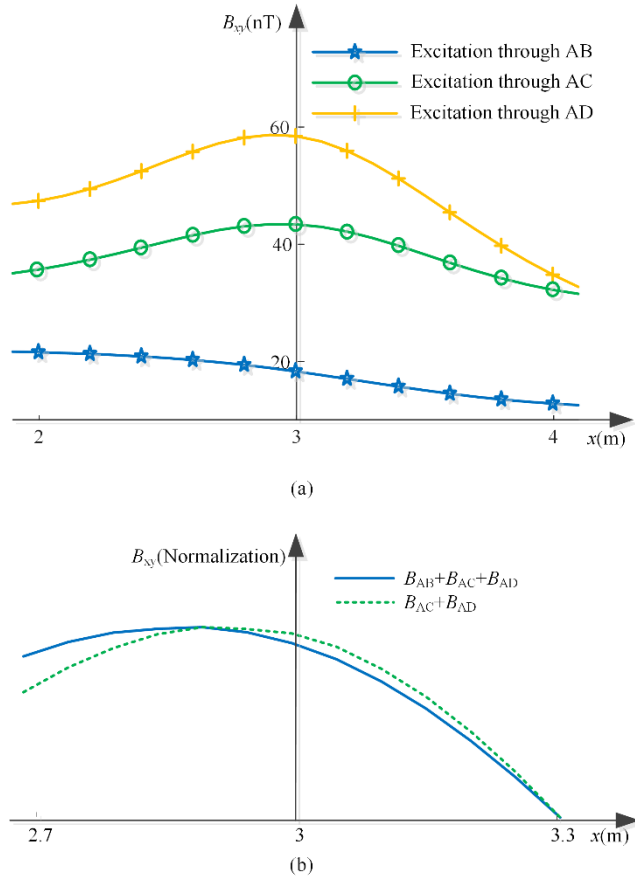


FIGURE 4. Amplitude magnitude of the magnetic field with different excitations and with different magnetic field superposition.

### III. METHODS FOR ACCUMULATING TOPOLOGICAL FEATURES UNDER COMBINED SOURCES

#### A. RECOGNITION OF TOPOLOGICAL TOP-HAT FEATURES

Mathematical morphology is a widely used image data processing technique [19] for edge detection and physical field feature detection of image data [20], [21]. The top-hat algorithm, a key player in image morphology, specializes in identifying bumps within an image and is commonly utilized in various domains such as frequency estimation [22], infrared detection [23], and medical image enhancement [24]. In the context of the magnetic induction intensity magnitude of the grounding grid in the image represented by  $f$ , the top-hat algorithm proves valuable for pinpointing the location of peak magnetic induction intensity. In image morphology, and are two fundamental operators, defined as follows:

$$(f \ominus b)(s, t) = \min\{f(s-x, t-y) - b(x, y) \mid (s-x, t-y) \in D_f; (x, y) \in D_b\} \quad (3)$$

$$(f \oplus b)(s, t) = \max\{f(s-x, t-y) + b(x, y) \mid (s-x, t-y) \in D_f; (x, y) \in D_b\} \quad (4)$$

In the given equation,  $b$  represents the structural probe, and the elements in the structural probe are often denoted as 0. The variables  $(s, t)$  correspond to the coordinates in

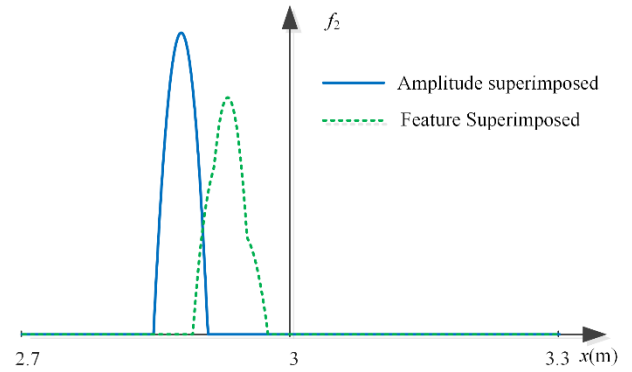


FIGURE 5. Topological characterization under two processing methods.

TABLE 1. Topological localization error with two processing methods for simulation data.

Processing Method	Maximum Error (mm)	Mean Error (mm)
Magnetic Field Superposition deals with $x = 3\text{m}$	125.0	57.3
Methods in this paper deals with $x = 3\text{m}$	79.0	41.3
Magnetic Field Superposition deals with $x = 6\text{m}$	291.0	109.5
Methods in this paper deals with $x = 6\text{m}$	192.0	70.6

the image, whereas  $(x, y)$  represents the coordinates in the structural probe.  $D_f$  denotes the definition domain of the image, and  $D_b$  represents the definition domain of the structural probe.

The morphology top-hat operation is defined as the outcome obtained by subtracting the original image from its morphological erosion, followed by dilation. The top-hat feature  $f_2$  of the grounding grid image can be represented as the localization of the grounding grid topology. A higher value of the top-hat feature indicates more prominent topological features in the grounding grid.

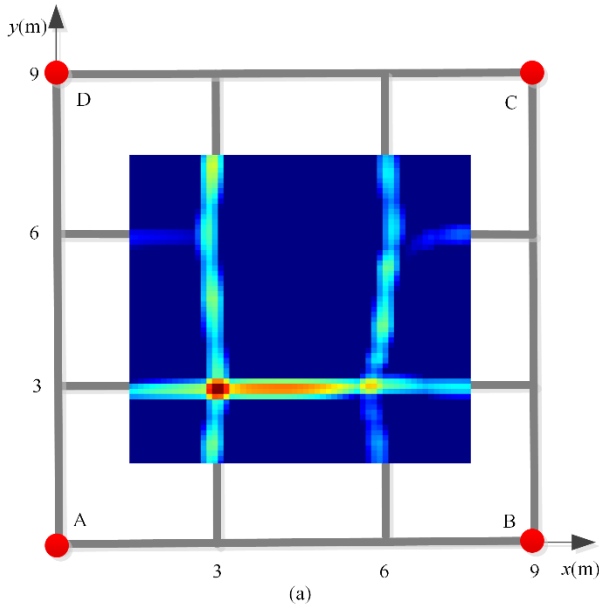
$$f_2 = f - (f \ominus b) \oplus b \quad (5)$$

#### B. IMAGING METHODS FOR ACCUMULATING TOPOLOGICAL FEATURES

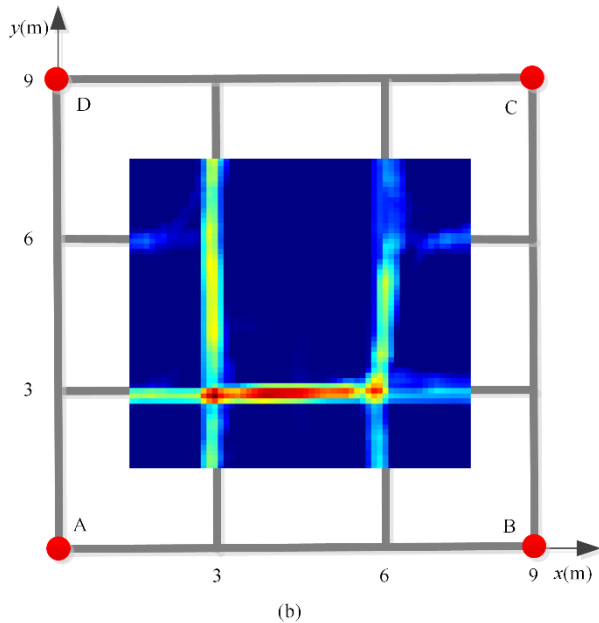
The traditional approach for handling the surface magnetic field of a combined source involves superimposing the magnetic induction intensities from various excitations and subsequently processing them. The calculation of topological feature  $f_3$  is expressed as follows:

$$f_3 = f(\sum B_f) - (f(\sum B_f) \ominus b) \oplus b \quad (6)$$

In the presence of breakpoints in the grounding grid topology, the superposition-before-recognition approach led to a more substantial shift in the grounding grid topology. To mitigate topology shifts under combined sources, a strategy is employed in which top-hat eigenvalues are computed individually for the magnetic induction strength under each set



(a)



(b)

FIGURE 6. Topology under two treatments (a) magnetic field superposition (b) feature superposition.

of excitations. Subsequently, these top-hat eigenvalues were superimposed before further processing.

$$f_3 = \sum f(B_f) - (f(B_f) \odot b) \oplus b \quad (7)$$

The magnetic induction intensity along the survey line was processed using the feature accumulation method, and the results are shown in Fig. 5. Observing the positions of the top-hat eigenvalues reveals that employing the feature accumulation method diminishes the topological localization offset compared with the approach of superimposing all magnetic fields. This method essentially combines the top-hat eigenvalues of the magnetic fields exhibiting peak features, excluding those without peak features from the superposition. This exclusion reduces the impact of invalid magnetic fields

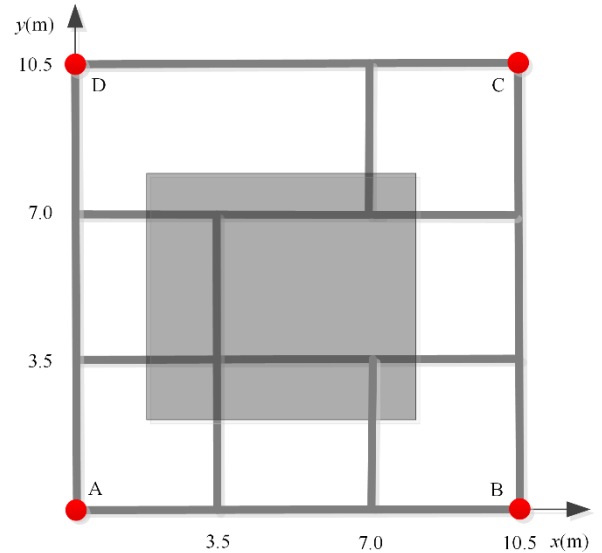


FIGURE 7. Physical modeling of the grounding grid.

TABLE 2. Topological localization error with two processing methods for experimental data.

Processing Method	Maximum Error (mm)	Mean Error (mm)
Magnetic Field Superposition deals with $x = 3.5\text{m}$	531.0	164.2
Methods in this paper deals with $x = 3.5\text{m}$	274.0	77.6
Magnetic Field Superposition deals with $x = 7\text{m}$	349.0	159.0
Methods in this paper deals with $x = 7\text{m}$	284.0	111.5

on the peak offset. It is crucial to note that although the feature accumulation result can mitigate the increase in offset caused by topological breakpoints, it does not entirely eliminate the topological localization offset. This is because the currents in the bypass branches contribute to an offset under each set of excitations.

### C. SIMULATION EXAMPLE

The topological characteristics of the grounding grid in Fig. 3 were discerned using magnetic field superposition and feature accumulation methods. The results of the identification process are shown in Fig. 6.

Upon analyzing the computation results, it is evident that both data processing methods exhibit a certain level of efficacy in recognizing the grounding grid topology. However, distinctions in local nuances were observed. Employing the magnetic field superposition method introduces an offset in the identification and localization of the grounding grid topology, particularly at the breakpoint location. As the proximity to the topological intersection ( $x = 3\text{m}$ ,  $y = 6\text{m}$ ) increases, the offset value of the topological localization became more pronounced. This phenomenon is attributed to the heightened influence of flat steel currents at  $x = 0\text{-}3\text{m}$ ,  $y = 6\text{m}$ , closer to the intersection point, resulting in a bending effect in the



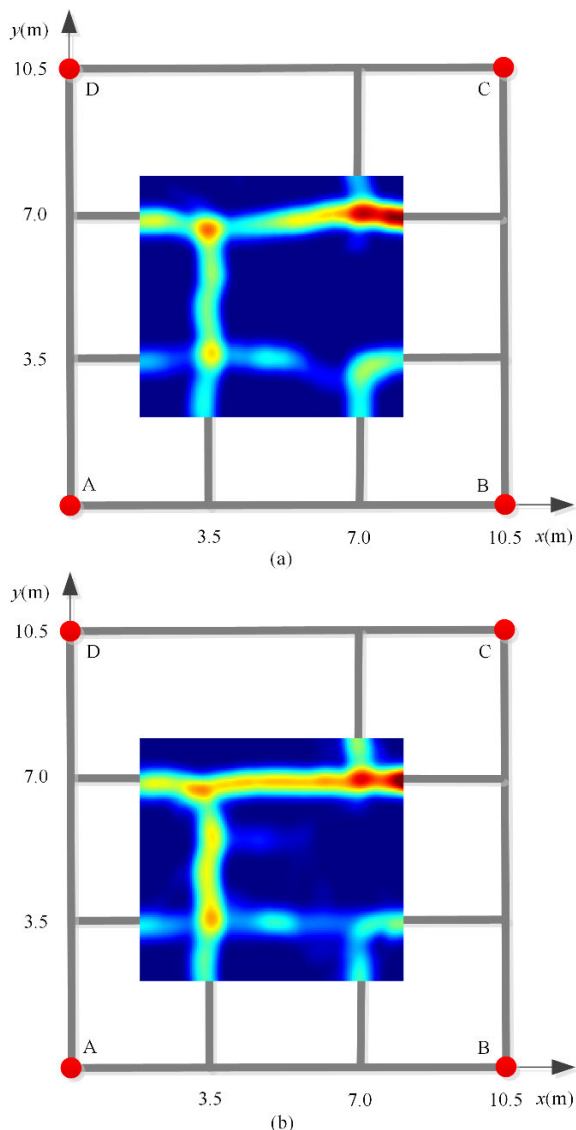


**FIGURE 8.** Topology under two processing methods (a) magnetic field superposition (b) feature superposition.

topology of the grounding grid at  $x = 3\text{m}$  and  $x = 6\text{m}$ , as depicted in Fig. 6(a).

In contrast, the feature accumulation method proved effective in reducing the offset caused by breakpoints, while maintaining a straight topology, as shown in Fig. 6(b). To quantitatively compare the offset sizes of the two methods in topological localization, positional deviations at  $x = 3\text{m}$  and  $x = 6\text{m}$  were calculated, and the results are presented in Table 1.

A comparison of the localization errors computed by the two methods reveals topological biases in both magnetic-field superposition and feature-accumulation techniques. However, the localization error from the feature accumulation method was smaller than that from the magnetic field superposition method, with a more concentrated error deviation. Consequently, the feature-accumulation method provides a more accurate representation of the grounding grid topology.

#### IV. EXPERIMENTAL ANALYSIS

As illustrated in Fig. 7 for the grounding grid topology model at the test site, the model comprises a  $3 \times 3$  grid with a grid side length of  $3.5\text{m}$  and a grid buried depth of  $0.8\text{m}$ . Four points, A, B, C, and D, located on the lead wire, serve as excitation points. Point A serves as the common point, and the excitation is sequentially injected in the order AB, AC, and AD. The induced voltage on the ground surface was collected using a coil sensor array.

To mitigate lead-wire interference, the data analysis focused exclusively on the shaded area in Fig. 7. The collected data were processed using the magnetic field superposition and feature accumulation methods. The results are shown in Fig. 8.

The results of the topological feature comparison reveal that both methods can identify the general topology; however, discrepancies in local locations exist. The magnetic field superposition method introduces a significant offset in the topological intersection points' locations, which shows obvious topological anomalies in the flat steel, such as at  $x = 6.0\text{--}7.0\text{m}$ ,  $y = 3.5\text{m}$ , and  $x = 3.5\text{--}7.0\text{m}$ ,  $y = 7.0\text{m}$  in Fig. 8(a).

To quantify the deviation magnitude between the results of the two methods, the topological location is computed by extracting data at  $y = 3.5\text{m}$  and  $y = 7.0\text{m}$ , respectively. The topological location errors are listed in Table 2.

In Table 2, the grounding grid topology localization deviation of the feature superposition method at both locations is smaller than that of the calculated results of the magnetic field superposition method. The feature superposition method demonstrates a higher accuracy in identifying the topology than the magnetic field superposition method, resulting in a grounding grid topology that is closer to the actual configuration.

While the experimental process is subject to larger errors owing to sensor positioning inaccuracies, the overall impact on the analysis of the comparison results is minimal.

#### V. CONCLUSION

In this study, we propose an improved method to address the increasing topological offset in combined source identification for small grounding grid topology detection. This method involves accumulating the topological features of the grounding grid under the excitation of combined sources. After theoretical analysis and test-field experiments, the following conclusions were drawn.

In a small grounding grid, the magnetic field generated by neighboring branch currents plays a significant role in topological localization. The traditional method of locating the peak magnetic field may result in a discrepancy between the calculated results and actual values, and this difference amplifies with increases neighboring branch current.

When a breakpoint occurs in the grounding grid topology, the difference between the neighboring branch currents near the breakpoint becomes more pronounced. At a given excitation, this difference reaches a maximum value, leading to the absence of an extreme value of magnetic induction strength

above the topology. The utilization of the magnetic field superposition processing method causes the peak position to deviate from the topology, thereby affecting the accuracy of topology localization.

Compared to the magnetic field superposition processing method, the feature accumulation processing method can eliminate the portion of local magnetic field data lacking extreme value features, thereby reducing the offset in topological localization. Simulation and test field experiments demonstrated that the topology feature accumulation method for grounded grids under combined source excitation is an effective optimization scheme that enhance the accuracy and precision of topology detection for small grounded grids.

## REFERENCES

- [1] H. Lin, H. Liu, Z. Zhang, X. Ma, Z. Yang, C. Wen, Y. Lu, M. Yan, and Y. Huang, "Evaluation and optimization of safety performance state of grounding grid," in *Proc. IEEE 4th Int. Electr. Energy Conf. (CIEEC)*, Wuhan, China, May 2021, pp. 1–4.
- [2] W. Xuming, L. Ning, Z. Qiaoyun, L. Hang, Z. Feng, H. Shengnan, and C. Menglu, "Analysis of safety index in substation considering the damage of external ground network," in *Proc. IEEE 6th Conf. Energy Internet Energy Syst. Integr. (EI2)*, Chengdu, China, Nov. 2022, pp. 658–663.
- [3] Z. Zhang, H. Ye, Y. Dan, Z. Duanmu, Y. Li, and J. Deng, "Novel method for comprehensive corrosion evaluation of grounding device," *IEEE Access*, vol. 8, pp. 72102–72111, 2020.
- [4] Q. Duan, S. Li, X. Yi, and H. Song, "Design of a grounding grid corrosion detection device based on the electrical network method," in *Proc. Int. Conf. Inf. Control, Electr. Eng. Rail Transit (ICEERT)*, Lanzhou, China, Oct. 2021, pp. 148–157.
- [5] Y. Hong, Z. Yu, Y. Hua, W. Qian, Z. Laifu, and X. Yudong, "Diagnosis means and development tendency of power economy grounding grid flaws," in *Proc. IEEE 4th Adv. Inf. Manage., Communicates, Electron. Autom. Control Conf. (IMCEC)*, vol. 4, Chongqing, China, Jun. 2021, pp. 740–746.
- [6] X. Yan, S. Huang, W. T. Smolik, W. Chen, and S. Yang, "A detection method for fast electrical impedance imaging of grounding grid based on optimized differential-multigrad-homotopy algorithm," *IEEE Trans. Instrum. Meas.*, vol. 72, pp. 1–14, 2023.
- [7] L. Kai, Y. Fan, Z. Songyang, Z. Liwei, H. Jiayuan, W. Xiaoyu, and I. Ullah, "Research on grounding grids imaging reconstruction based on magnetic detection electrical impedance tomography," *IEEE Trans. Magn.*, vol. 54, no. 3, pp. 1–4, Mar. 2018.
- [8] X. Xu, W. Wang, L. Li, and Y. Wang, "Fault diagnosis and improvement of substation grounding network in substation engineering based on video image recognition," in *Proc. IEEE 15th Int. Conf. Comput. Intell. Commun. Netw. (CICN)*, Bangkok, Thailand, Dec. 2023, pp. 1–7.
- [9] C. Lu, T. Zhang, S. Sun, Z. Cao, M. Xin, G. Fu, T. Wang, and X. Wang, "Fault diagnosis of tower grounding conductor based on the electromagnetic measurement and neural network," *IEEE Trans. Instrum. Meas.*, vol. 71, pp. 1–9, 2022.
- [10] H. Zhong, J. Liu, M. Tang, J. Zhang, K. Liu, S. Xiao, and Y. Guo, "The influence analysis of the power grid topology on the stray current invading transformers," in *Proc. 4th Int. Conf. Control Robot. (ICCR)*, Guangzhou, China, Dec. 2022, pp. 179–182.
- [11] N. Permal, M. Osman, A. M. Ariffin, and M. Z. A. A. Kadir, "The impact of substation grounding grid design parameters in non-homogenous soil to the grid safety threshold parameters," *IEEE Access*, vol. 9, pp. 37497–37509, 2021.
- [12] W. Wang, H. Zhang, B. Xie, and C. Liu, "Research on corrosion detection system of substation grounding grid based on non-contact measurement," in *Proc. IEEE 6th Adv. Inf. Technol., Electron. Autom. Control Conf. (IAEAC)*, Beijing, China, Oct. 2022, pp. 1933–1936.
- [13] A. Qamar, I. H. Al-Kharsan, Z. Uddin, and A. Alkhayyat, "Grounding grid fault diagnosis with emphasis on substation electromagnetic interference," *IEEE Access*, vol. 10, pp. 15217–15226, 2022.
- [14] W. D. Wang, X. Q. Hu, Z. Y. Xu, H. W. Wang, and Z. H. Fu, "Topology detecting method of grounding grids based on morphological filtration," *Trans. China Electrotechnical Soc.*, vol. 36, no. 17, pp. 3685–3692, Oct. 2020.
- [15] Y. Fan, L. Kai, Z. Liwei, Z. Songyang, H. Jiayuan, W. Xiaoyu, and G. Bin, "A derivative-based method for buried depth detection of metal conductors," *IEEE Trans. Magn.*, vol. 54, no. 4, pp. 1–9, Apr. 2018.
- [16] Z. Fu, S. Song, X. Wang, J. Li, and H.-M. Tai, "Imaging the topology of grounding grids based on wavelet edge detection," *IEEE Trans. Magn.*, vol. 54, no. 4, pp. 1–8, Apr. 2018.
- [17] W. D. Wang, "Research on detecting method and equipment of grounding grids structure using combined pulse source electromagnetic method," M.S. thesis, School Elect. Eng., Chongqing Univ., Chongqing, China, 2021.
- [18] W. G. TIAN, L. L. Liu, X. Liao, J. Zhang, H. W. Wang, and Z. H. Fu, "Combined source magnetic field superposition imaging detection method for grounding grid topology," *J. Chongqing Univ.*, vol. 46, no.11, pp. 90–101, May 2023.
- [19] D. Celeita, J. D. Perez, and G. Ramos, "Assessment of a decaying DC offset detector on CTs measurements applying mathematical morphology," *IEEE Trans. Ind. Appl.*, vol. 55, no. 1, pp. 248–255, Jan. 2019.
- [20] S. Li, Y. Linlin, and L. Xinxin, "Algorithm of Canny operator edge pre-processing based on mathematical morphology," in *Proc. Int. Conf. Comput. Eng. Appl. (ICCEA)*, Guangzhou, China, Mar. 2020, pp. 349–352.
- [21] Y. Gu, W. Tang, and Z. YU, "Feature analysis of overvoltage in offshore wind farms using mathematical morphology," in *Proc. 5th Asia Conf. Power Electr. Eng. (ACPEE)*, Chengdu, China, Jun. 2020, pp. 129–133.
- [22] I. G. N. A. D. Saputra, I. G. A. M. Sunaya, I. B. Sugirianta, and I. G. N. B. C. Bawa, "Combination of top-hat and bottom-hat transforms for frequency estimation," in *Proc. Int. Conf. Appl. Sci. Technol. (ICAST)*, Manado, Indonesia, Oct. 2018, pp. 687–692.
- [23] L. Deng, G. Xu, J. Zhang, and H. Zhu, "Entropy-driven morphological top-hat transformation for infrared small target detection," *IEEE Trans. Aerosp. Electron. Syst.*, vol. 58, no. 2, pp. 962–975, Apr. 2022.
- [24] H. Ruiying, "Method of medical image segmentation based on chan-vese model," in *Proc. IEEE Int. Conf. Adv. Electr. Eng. Comput. Appl. (AEECA)*, Dalian, China, Aug. 2022, pp. 697–701.

**XIZHE ZHANG** was born in 1988. He received the M.S. degree. He is currently with State Grid Tianjin Electric Power Company. His research interests include electrical engineering and automation and control engineering.

**BEN YU** was born in 1990. He received the M.S. degree. He is currently with the Electric Power Research Institute, State Grid Tianjin Electric Power Company. His research interests include electrical engineering and automation and control engineering.

**LONGHUAN LIU** was born in 1995. He received the master's degree in electrical engineering from Chongqing University, in 2020, where he is currently pursuing the Ph.D. degree. His research interests include transient electromagnetic data processing, buried pipeline corrosion detection, and grounding grid corrosion detection.

**ZHIHONG FU** received the B.S. degree in applied geophysics from China University of Geosciences, Wuhan, China, in 1987, and the M.S. and Ph.D. degrees in electrical engineering from Chongqing University, Chongqing, China, in 2001 and 2007, respectively. He is currently a Professor with the Department of Electrical Engineering, Chongqing University. His current research interests include electromagnetic surveying and electric energy metering.

**JINSHAN YU** was born in 1979. He received the M.S. degree. He is currently with the Electric Power Research Institute, State Grid Tianjin Electric Power Company. His research interest includes corrosion and protection of materials.

**XIN CHENG** was born in 1999. His research interests include grounding network topology and corrosion fracture detection.

...